

Magnetic properties and microstructures of Fe–Pt thin films sputter deposited under partial nitrogen gas flow

C. Y. You,^{a)} Y. K. Takahashi, and K. Hono
National Institute for Materials Science, Tsukuba 305-0047, Japan

(Received 17 September 2004; accepted 9 May 2005; published online 5 July 2005)

Continuous Fe_{100-x}Pt_x thin films ($x=44, 50, 56, 60,$ and 65) with a thickness of around 80 nm were prepared by dc magnetron sputtering under a mixture of argon and nitrogen gases. The maximum coercivity was obtained at the Fe₅₆Pt₄₄ off-stoichiometric composition after postannealing for $L1_0$ ordering. For the equiatomic and Pt-rich films, partial nitrogen flow during sputtering deteriorated the in-plane coercivity of the postannealed samples due to conglomeration of smaller grains and the presence of $L1_2$ FePt₃ phase. After postannealing for $L1_0$ ordering, the Fe-rich films grown in argon and mixture of argon and nitrogen atmospheres are both composed of $L1_0$ fct phase only, and the enhancement of the degree of order and strong preferential in-plane alignment of the c axis in the presence of nitrogen causes in-plane coercivity increase. By introducing nitrogen during sputtering, an in-plane coercivity of 1303 kA/m (16.4 kOe) was obtained for the continuous Fe₅₆Pt₄₄ thin film annealed at 700 °C. © 2005 American Institute of Physics. [DOI: 10.1063/1.1943509]

I. INTRODUCTION

The magnetic properties of $L1_0$ -type FePt thin films have been studied intensively, because they are considered to have potential application as thin-film magnets for microelectronic machine systems (MEMSs), high-performance magnets for dental applications, and ultrahigh-density recording media.¹⁻⁷ Although the $L1_0$ -ordered FePt phase has a large magnetocrystalline anisotropy of 7×10^7 ergs/cc,¹ the coercivity varies in a wide range from a few hundreds to 3819 kA/m (48 kOe), depending largely on their microstructures. Yung *et al.*² obtained a coercivity of 955 kA/m (12 kOe) and an energy product of 120 kJ/m³ from the FePt thin films prepared by sputtering and postannealing above 400 °C. Liu *et al.*³ reported coercive forces higher than 796 kA/m (10 kOe) by rapidly annealing an Fe/Pt multilayered thin film, and achieved maximum-energy products of higher than 320 kJ/m³ (40 MGOe) at room temperature. Watanabe and Homma⁸ reported a high coercivity of about 621 kA/m (7.8 kOe) for the FePt thin films deposited on a Pt underlayer, and it was later shown that this high coercivity was possibly linked with the multitwins that were introduced from the Pt/FePt interfaces.⁹ Goto *et al.* reported a large coercivity of 3819 kA/m (48 kOe) in very thin islandlike grown films, but its coercivity decreases when the film thickness increases.¹⁰ Shima *et al.*¹¹ and Okamoto *et al.*¹² also reported a very large coercivity for particulate films epitaxially grown on heated MgO single-crystal substrates, but their coercivity drops drastically to about 160 kA/m (2 kOe) when the film becomes continuous after growing to a thickness of more than 40 nm, as originally reported by Goto *et al.*¹⁰ This is because there are few domain-wall pinning sites in the single crystalline films. To achieve high coercivity in continuous FePt thin films, Takahashi *et al.* introduced a number of domain-wall pinning sites by fabricating nano-

sized polycrystalline continuous films of about 100 nm in thickness, and obtained an in-plane coercivity of 1035 kA/m (13 kOe).¹³

As processing parameters for fabricating high coercive FePt films, various gas atmospheres such as oxygen and nitrogen were also tested.¹⁴⁻¹⁶ Among these, a recent study by Wang *et al.* reported that the in-plane hard magnetic properties of the Fe₅₆Pt₄₄ thin films can be improved by reactive rf magnetron sputtering in an argon and nitrogen atmosphere,¹⁶ in which the highest in-plane coercivity of 1154 kA/m (14.5 kOe) was reported. Although they speculated that the increase of the coercivity was due to the formation of iron nitride and enhanced chemical ordering, the mechanism of the nitrogen effects was not revealed because of the limited structural analysis investigation. It was also reported that the incorporated N atoms in the as-deposited films had been released from the ordered fct phase during annealing.¹⁶

In this work, we focused on the effect of nitrogen on the microstructure and magnetic properties of Fe_xPt_{100-x} thin films prepared by reactive dc magnetron sputtering under argon gas or a mixture of argon and nitrogen gases. The microstructure of the films was investigated by x-ray diffraction (XRD) and transmission electron microscopy (TEM). The main purpose of this work was to understand the mechanism of the coercivity increase by the nitrogen addition, and to explore the possibility of developing high-performance FePt thin-film magnets. By introducing nitrogen during sputtering, an in-plane coercivity of 1303 kA/m (~16.4 kOe) was obtained for the continuous Fe₅₆Pt₄₄ thin film with a thickness of around 80 nm, about 20% higher than in a similar film deposited under argon.

II. EXPERIMENTS

Fe_xPt_{100-x} ($x=44, 50, 56, 60,$ and 65) films were prepared by codeposition of Fe and Pt on thermally oxidized Si wafers using a multiple-target dc-sputtering system with high-purity targets of 99.99% Fe and 99.9% Pt at room tem-

^{a)}Author to whom correspondence should be addressed; electronic mail: caiyin.you@nims.go.jp

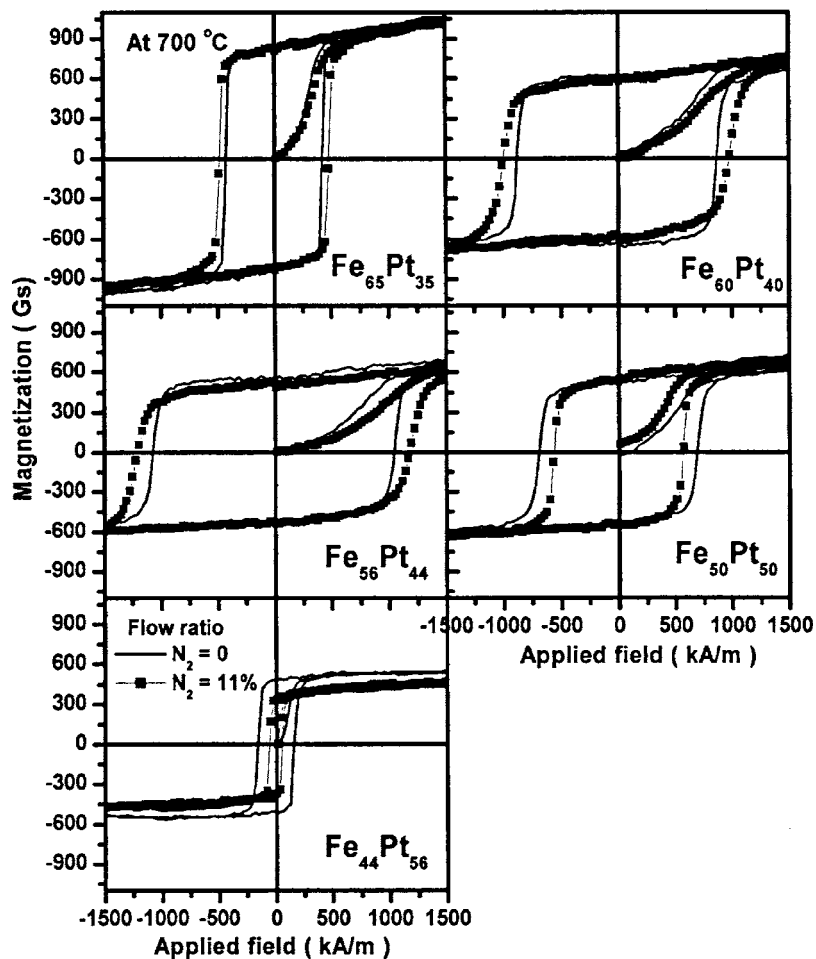


FIG. 1. In-plane hysteresis loops of thin films annealed at 700 °C.

perature. The base pressure of the system was better than 2×10^{-7} Pa. High-purity mixed gases of 0.1 Pa with different N_2 ratios (0, 11%) were flown during sputtering. The substrate was attached to a rotating table. The composition of the thin films was modified by adjusting the target power. The thicknesses of the thin films were controlled to be around 80 nm. Postdeposition annealing was performed in vacuum of better than 5×10^{-4} Pa at various temperatures for 15–60 min by sealing the samples in quartz tubes and putting them into a preheated muffle furnace. The phase constituents of the films were examined by (θ -2 θ) XRD using $Cu\ k_\alpha$ radiation. The microstructure of the films was examined by TEM, Philips CM200, and JEOL 2010F TEMs. The compositions of the films were estimated by energy dispersive x-ray spectroscopy. A vibrating-sample magnetometer (VSM) with a maximum applied field of 2 T and a superconducting quantum interface device (SQUID) magnetometer with a maximum applied field of 5.5 T was used for measuring magnetic properties along the in-plane direction. Some of the samples were also measured along the out-of-plane direction.

III. RESULTS

A. Magnetic properties

By annealing above 600 °C, the ordering from the $A2$ structure to the $L1_0$ structure took place and the films became magnetically hard. Figure 1 shows typical in-plane hysteresis

loops of the Fe_xPt_{100-x} ($x=44, 50, 56, 60,$ and 65) films annealed at 700 °C for 30 min. The lines without the square marks and with the square marks indicate the magnetization curves for the films deposited under argon and mixed gases with partial nitrogen flow, respectively. Although coercivity was enhanced with the presence of nitrogen in the case of Fe-rich compositions, nitrogen has an adverse effect in the case of equiatomic and Fe-poor compositions. It was also found that no magnetic hardening was achieved even by annealing at 800 °C for the $Fe_{44}Pt_{56}$ film with a partial nitrogen flow and the saturation magnetization was significantly lower than the corresponding film grown in the argon atmosphere, as shown in Fig. 1.

Figure 2 summarizes the in-plane coercivity of the films of various compositions annealed for 30 min at three different temperatures. At all temperatures, the same trends can be seen in the coercivity, i.e., the coercivity was enhanced with nitrogen only for the Fe-rich compositions. The highest coercivity was obtained from the $Fe_{56}Pt_{44}$ film annealed at 700 °C: 1075 kA/m for the film sputtered under argon and 1207 kA/m for the film sputtered under 11% nitrogen flow. By using SQUID with the maximum external applied field of 5.5 T, the highest coercivity of 1303 kA/m was recorded from the $Fe_{56}Pt_{44}$ film that was sputter deposited under 11% nitrogen flow after annealing at 700 °C for 30 min [marked in Fig. 2(b) by a circle]. The changes of coercivity with composition are mainly attributed to the anisotropy variations due to the dependences of the degree of order on

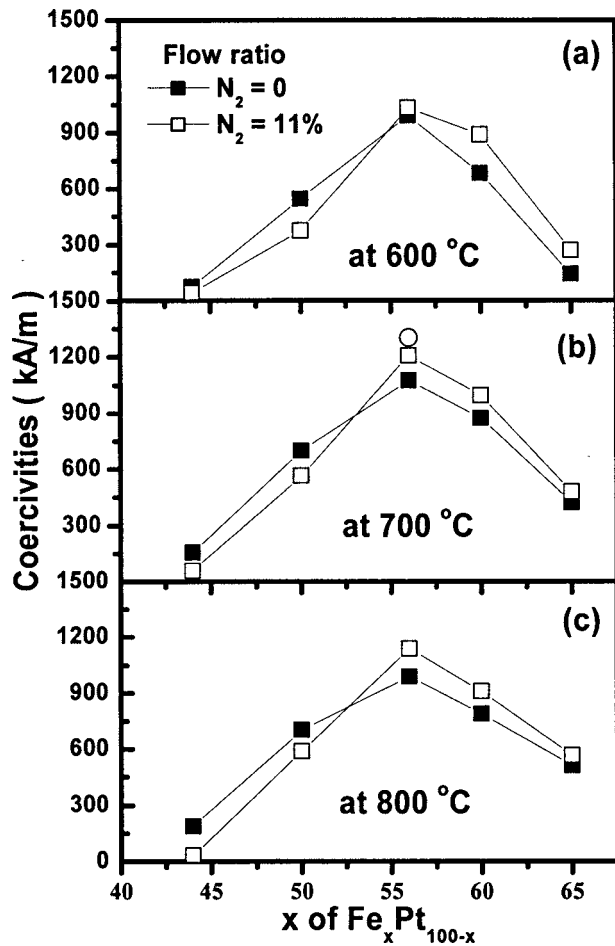


FIG. 2. In-plane coercivity of thin films annealed at various temperatures for 30 min.

compositions.¹⁷ Figure 3 shows the coercivity of the $\text{Fe}_{65}\text{Pt}_{35}$ and $\text{Fe}_{56}\text{Pt}_{44}$ films as functions of annealing time at 700 °C. The coercivity increases drastically after annealing for 15 min and the coercivity of the films grown in the partial nitrogen flow is higher than the ones grown in the argon atmosphere. The coercivity of the $\text{Fe}_{56}\text{Pt}_{44}$ film slightly decreases after annealing longer than 30 min, while that of $\text{Fe}_{65}\text{Pt}_{35}$ does not show much change within the range of annealing time.

B. Preferred orientations and phase evolutions (XRD)

Figure 4(a) shows the XRD profiles of the as-deposited films grown in the argon atmosphere, in which the preferred orientation of $\{111\}$ in the plane is predominant. It is well known that the growth of films with preferred orientation is closely related to surface energy, interface energy, and strain energy.^{18–20} The $[111]$ preferential orientation observed in Fig. 4(a) can be explained from the lowest surface energy of the fcc $\{111\}$ plane. When nitrogen was introduced during sputtering, the growth direction of the thin films changed. The XRD profiles of the as-deposited films under an 11% flow ratio of nitrogen are shown in Fig. 4(b). Unlike in a previous report,¹⁶ the formation of iron nitride is not detected here. Compared with Fig. 4(a), the $\{200\}$ diffraction peak appears and becomes stronger with increasing the Fe content

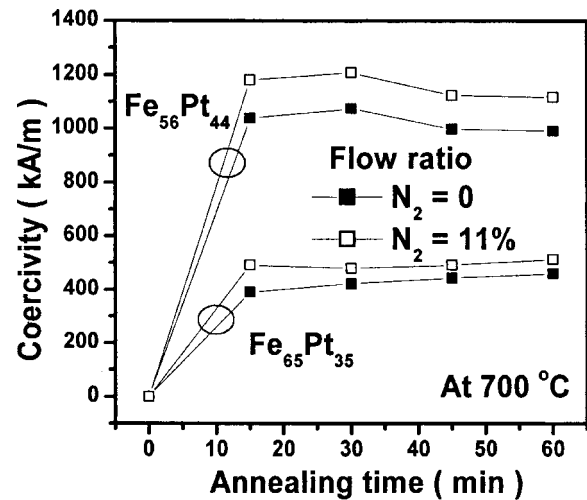


FIG. 3. In-plane coercivity dependences on annealing time for the films $\text{Fe}_{65}\text{Pt}_{35}$ and $\text{Fe}_{56}\text{Pt}_{44}$.

of the films. This indicates that the surface energy, interfacial energy, or strain energy might have been altered by the nitrogen flow during sputtering.^{18–20} Figure 4(c) shows the lattice parameter a of the as-deposited films determined from the $\{111\}$ plane diffraction. It is apparent that the crystalline lattice was expanded by nitrogen flow, so N atoms are thought to be dissolved interstitially in the disordered fcc phase. Since the interstitial dissolution of N expands the lattice of FePt, the strain energy would be very different from that for the N-free film, resulting in the development of a different preferred orientation of the grains.

In order to investigate the effects of nitrogen interstitial atoms on the microstructure of the annealed films, XRD (θ - 2θ) scans of the films annealed at 800 °C are shown in Figs. 5(a) and 5(b) for the films grown in the argon atmosphere and 11% partial flow of nitrogen, respectively. Based on the magnetic hardening shown in Fig. 2, all diffraction peaks can be indexed as the $L1_0$ -ordered FePt phase except for the ones from the substrate. It is obvious that the annealed films inherit the preferred orientation of the as-deposited films. All annealed films grown in the argon atmosphere show strong $[111]$ preferred orientation except for the $\text{Fe}_{50}\text{Pt}_{50}$ film, which means that films with both Fe-rich and Pt-rich compositions exhibit $[111]$ preferred orientation. On the other hand, the Fe-rich films grown in the partial nitrogen flow exhibit preferred growth of the $\{200\}$ planes as indicated by the higher intensity of the $\{200\}$ diffraction peak compared with randomly orientated polycrystalline structures. The preferred orientation of $\{200\}$ diffraction becomes stronger with increasing Fe concentration. But the presence of other diffraction peaks such as $\{001\}$ and $\{111\}$ indicates imperfect texture in comparison with the Fe-rich films grown under argon atmosphere. In order to investigate the behavior of interstitial nitrogen during annealing, the lattice parameter a of the thin films grown in the partial nitrogen was evaluated before and after annealing, as shown in Fig. 5(c). It can be seen that lattice parameter a was reduced after annealing. The lattice parameter a should be expanded due to the distortion of the c -axis direction during the ordering process. So

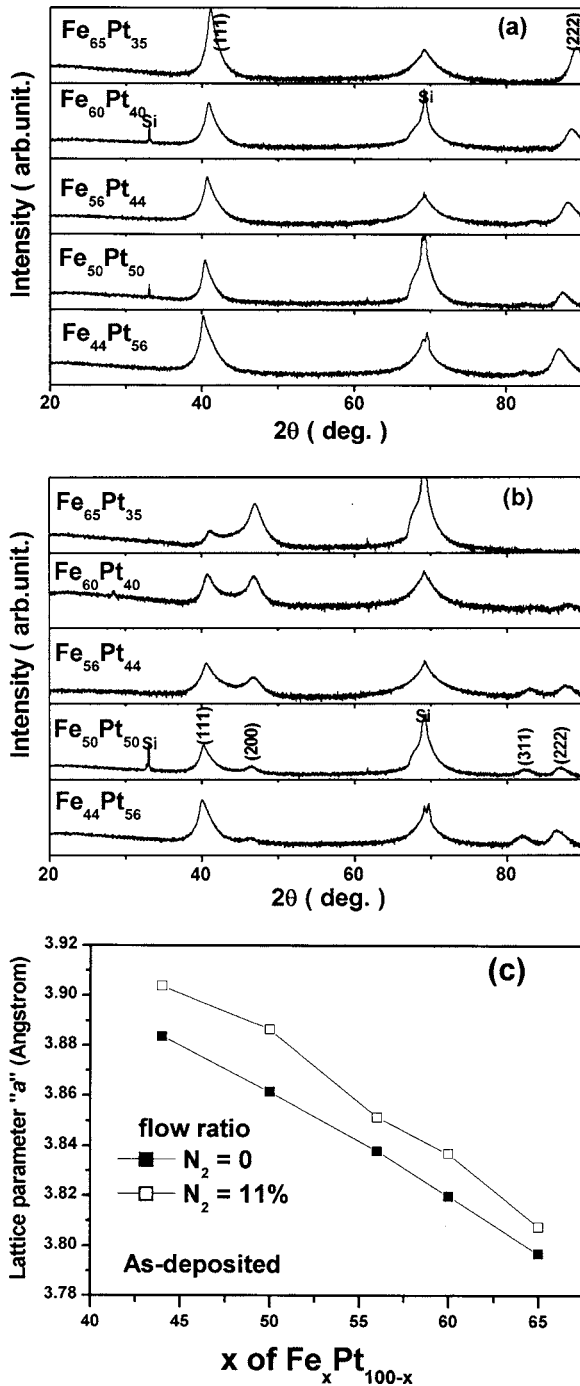


FIG. 4. XRD profiles of as-deposited thin films (a) in the argon atmosphere and (b) in the partial nitrogen flow, and lattice parameter a (c).

the shrinking of lattice a is mainly attributed to the releasing of N interstitial atoms from the ordered fct phase, in agreement with the previous report.¹⁶

The presence of interstitial nitrogen is expected to give some effects on the degree of order. Since $L1_0$ FePt has the tetragonal structure, the c/a ratio will represent the degree of order because the correct occupation of a higher fraction of Pt atoms results in a bigger difference of lattice constants a and c .^{21,22} The c/a of fully ordered stoichiometric FePt is 0.9639,²³ and that for completely disordered fcc FePt or ordered $L1_2$ -type fcc structure is 1. Based on the XRD peaks of the samples annealed at 800 °C, the approximate lattice ratio

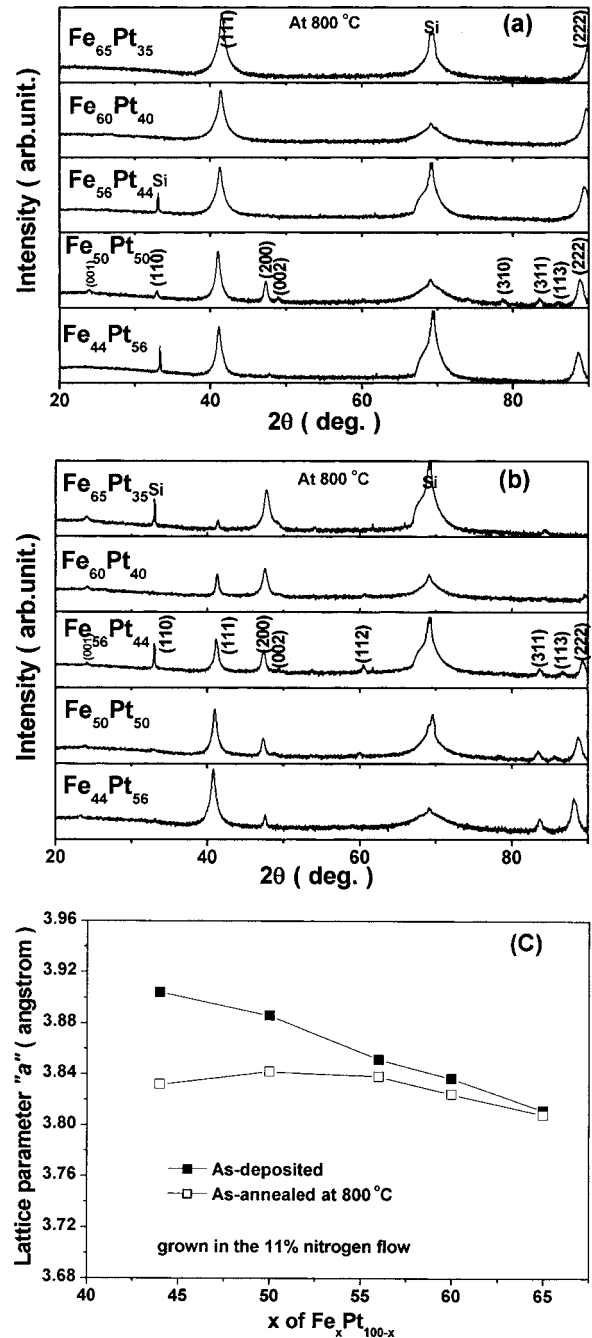


FIG. 5. XRD profiles of films annealed at 800 °C grown (a) in the argon atmosphere and (b) in the partial nitrogen flow; (c) the changes of the lattice parameter a of films grown in the partial nitrogen flow.

was evaluated as shown in Fig. 6. The c/a value of the $\text{Fe}_{60}\text{Pt}_{40}$ and $\text{Fe}_{65}\text{Pt}_{35}$ thin films could not be evaluated from the XRD patterns because of the strong texture. The inset of Fig. 6 shows the consistent results evaluated from selected area electron-diffraction (SAED) patterns taken from TEM specimens, which show the lower value of c/a for the Fe-rich $\text{Fe}_{60}\text{Pt}_{40}$ and $\text{Fe}_{56}\text{Pt}_{44}$ films after introducing partial nitrogen flow. From Fig. 5(c), most N interstitial atoms would be released from the ordered fct phase during annealing. Even if some N interstitial atoms were still present, these should result in an increase of the c/a ratio due to the drastic expansion of the c axis.²⁴ So the decrease of the c/a ratio can be reasonably attributed to the improved degree of order.

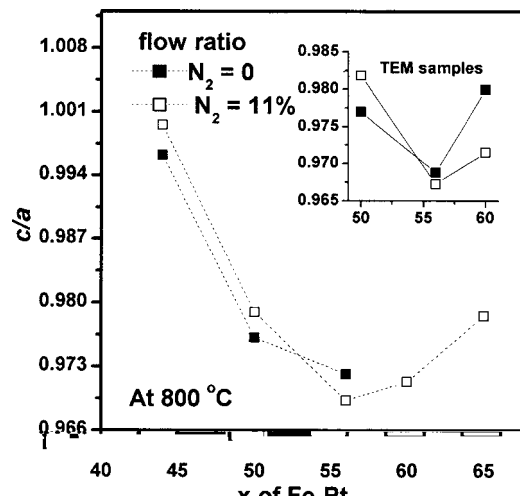


FIG. 6. The changes of the c/a values of samples by partial nitrogen flow.

From the value of c/a , we can conclude that the degree of order of the $\text{Fe}_{56}\text{Pt}_{44}$ and $\text{Fe}_{60}\text{Pt}_{40}$ thin films was enhanced by introducing nitrogen during sputtering. But the degree of order was possibly deteriorated by the partial nitrogen flow for the $\text{Fe}_{50}\text{Pt}_{50}$ and $\text{Fe}_{44}\text{Pt}_{56}$ thin films, which will be discussed in the Discussions section. The c/a value of the $\text{Fe}_{44}\text{Pt}_{56}$ thin film with nitrogen flow is close to 1, which implies that the formed phases change from the $L1_0$ phase to the antiferromagnetic $L1_2\text{FePt}_3$ phase,²⁵ in agreement with the observation of no magnetic hardening by annealing at 800 °C, as shown in Fig. 2. This is also reflected from the magnetic hysteresis in Fig. 1, in which the saturated magnetization of the $\text{Fe}_{44}\text{Pt}_{56}$ thin film significantly decreases after introducing nitrogen flow.

C. TEM observations

Figures 7(a) and 7(b) show the bright field images of the $\text{Fe}_{50}\text{Pt}_{50}$ films that were deposited in the argon atmosphere and the partial nitrogen atmosphere, respectively, and subsequently annealed at 600 °C for 30 min. Note that the in-plane coercivity of the film grown in nitrogen flow was lower by about 200 kA/m than that grown in argon, as shown in Fig. 2(a). The insets are the corresponding SAED patterns. All diffraction rings can be indexed as the $L1_0$ phase, in which the superlattice reflection (001) is marked by an arrow. For the $\text{Fe}_{50}\text{Pt}_{50}$ film, nitrogen flow makes the microstructure less homogeneous, in which some smaller grains aggregate in some areas. The size of these smaller grains is approximately 15 nm, which is comparable to the exchange length of the $L1_0$ FePt phase. This will cause averaging of magnetocrystalline anisotropy and will deteriorate the coercivity.²⁶ In order to characterize these smaller grains, the compositions of big and small grains were estimated by energy dispersive x-ray spectroscopy (EDS). It was found that some of the small grains possess much higher Pt content (around 60 at. %) than the equiatomic composition, while the composition of the big grains was close to the equiatomic composition. Considering the balance of the film composition, there exist some grains with higher Fe content. On the other hand, the compositions of all detected grains in the film grown in

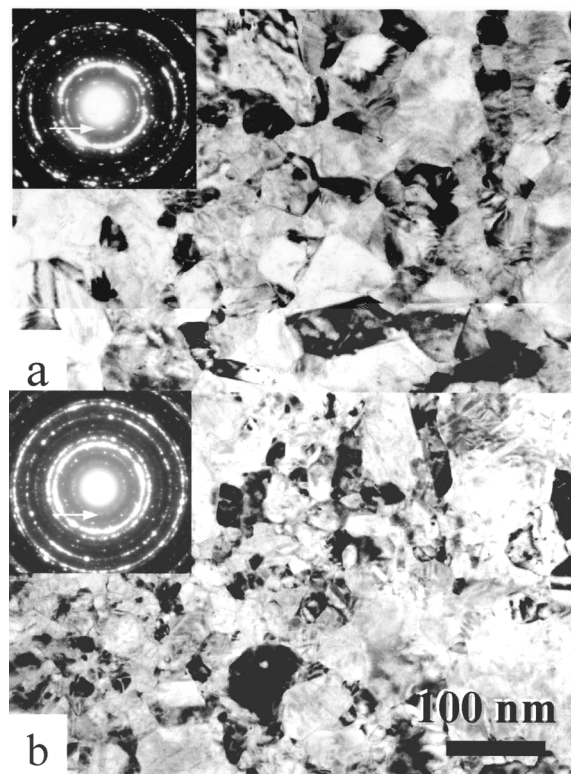


FIG. 7. The TEM bright field images of the $\text{Fe}_{50}\text{Pt}_{50}$ thin films annealed at 600 °C grown (a) in the argon atmosphere and (b) in the partial nitrogen flow.

the argon atmosphere are close to the equiatomic composition. So the composition fluctuation during annealing is concluded to be the effects of the interstitial nitrogen in the as-deposited film. By using a Gatan imaging filter, an inhomogeneous Fe map was observed (not shown here), in which Fe-poor grains are observed in agreement with the EDS results. From the equilibrium phase diagram of the Fe–Pt binary system,²⁵ a Pt content higher than 50 at. % Pt is beneficial for the formation of the $L1_2\text{FePt}_3$ phase. A large amount of the $L1_2\text{FePt}_3$ phase was also confirmed in the $\text{Fe}_{44}\text{Pt}_{56}$ film grown in the partial nitrogen flow. Since the FePt_3 phase is antiferromagnetic, the formation of this phase would decrease the volume fraction of the $L1_0$ -ordered phase, deteriorating the coercivity of the film.

In contrast, the in-plane coercivity was enhanced for the $\text{Fe}_{56}\text{Pt}_{44}$ film by partial nitrogen flow during sputtering. The bright field images of the samples annealed at 700 °C are shown in Figs. 8(a) and 8(b), respectively, for the films grown in the argon atmosphere and the partial nitrogen flow. Grain-size distribution profiles for both samples are shown in Fig. 8(c). The average grain size (around 58 nm) of the film grown under nitrogen flow is slightly larger than that grown in argon (around 54 nm), in agreement with previous results.¹⁶ So the coercivity enhancement by nitrogen flow cannot be attributed to the grain refinement. The TEM images of the $\text{Fe}_{60}\text{Pt}_{40}$ films, which also show coercivity enhancements by partial nitrogen flow, are consistent with the results obtained for the other films (not shown here).

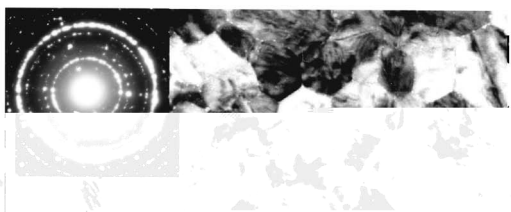


FIG. 8. The TEM bright field images of the $\text{Fe}_{56}\text{Pt}_{44}$ thin films annealed at 700°C grown (a) in the argon atmosphere and (b) in the partial nitrogen flow, and (c) the grain size distribution of annealed samples.

IV. DISCUSSIONS

This work has shown that the nitrogen flow during sputtering has important effects on the coercivity of the post-annealed $\text{Fe}_{100-x}\text{Pt}_x$ thin films ($x=44, 50, 56, 60,$ and 65) and these effects depend on the compositions of the films. The enhancement of coercivity by nitrogen flow during sputtering was observed only in the films with Fe-rich composition. The coercivity was deteriorated by nitrogen flow in the $\text{Fe}_{50}\text{Pt}_{50}$ and $\text{Fe}_{44}\text{Pt}_{56}$ films. The microstructural parameters such as grain size, degree of order, phase constituents, and crystallographic texture are thought to influence the coercivity of the films, so the question is which of these parameters are altered by nitrogen flow.

As for the $\text{Fe}_{56}\text{Pt}_{44}$ film, no significant change in grain size is observed by introducing nitrogen, as shown in Fig. 8. However, the XRD profiles in Fig. 5 indicate that the films

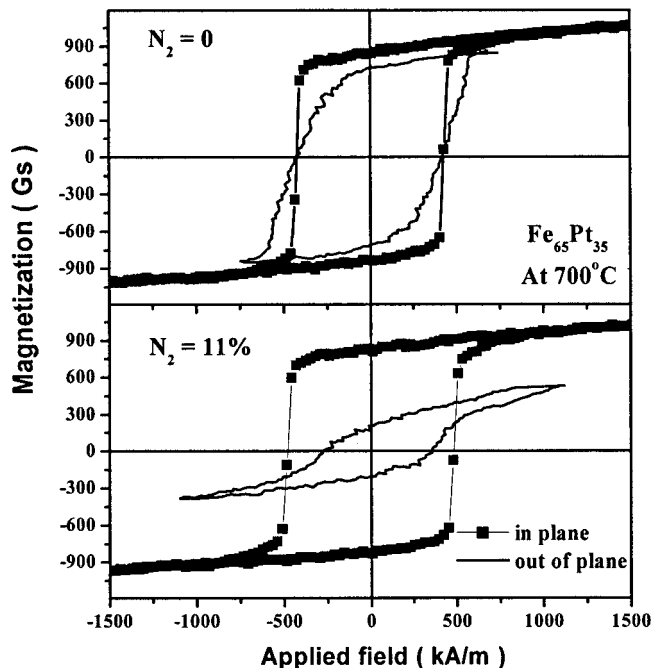


FIG. 9. The comparison of hysteresis loops with the fields parallel and perpendicular to the film plane for the $\text{Fe}_{65}\text{Pt}_{35}$ film.

grown in the partial nitrogen flow has preferred orientation lying in $\{200\}$ planes in the film plane unlike the films grown in the argon flow, which show a strong preferred orientation of $\{111\}$ in the film plane. Figure 9 shows magnetic hysteresis loops along the in-plane direction and out-of-plane direction for the $\text{Fe}_{65}\text{Pt}_{35}$ films without and with partial nitrogen flow annealed at 700°C . For the $\text{Fe}_{65}\text{Pt}_{35}$ film under argon atmosphere, the hysteresis loops in both geometries are similar, giving the same coercivity due to the c -axis tilting out of the film plane. The differences of loop shapes are mainly from the different angle of the c axis from the film plane ($\sim 35^\circ$) and normal direction to the film plane ($\sim 65^\circ$). For the $\text{Fe}_{65}\text{Pt}_{35}$ film under the mixed atmosphere of argon and nitrogen, the c axis mainly lie in plane due to the strong preferred orientation of $\{200\}$ in the film plane, which make it difficult to magnetize along the out-of-plane direction, resulting in a smaller out-of-plane coercivity. This indicates that preferred orientation has an influence on the coercivity. Moreover, the c axis along the film plane results in the high in-plane coercivity. However, the preferential growth of $\{200\}$ plane is enhanced as Fe concentration increases and the coercivity decreases with increasing Fe concentration. So the preferential alignment alone cannot explain the high coercivity in the $\text{Fe}_{56}\text{Fe}_{44}$ film grown in nitrogen. Another possible explanation for the coercivity change in the films is the degree of order. There are strong correlations between coercivity and chemical ordering, since the magnetocrystalline anisotropy depends on chemical ordering.²⁷⁻²⁹ Higher chemical ordering results in higher anisotropy and coercivity.^{21,22,27-29} Figure 6 shows that a smaller value of c/a is achieved in the $\text{Fe}_{56}\text{Pt}_{44}$ film deposited with partial nitrogen flow, indicating a higher degree of chemical long-range order.

The initial magnetization curves in Fig. 1 suggest that

the coercivity mechanism is dominantly domain-wall pinning. With respect to the randomly orientated grains, the intensity ratio of $\{111\}$ to $\{200\}$ diffractions is 100:38.²³ As shown in Fig. 5, the Fe-rich samples grown in the argon atmosphere show pure $\{111\}$ texture. In comparison with the films grown in the argon atmosphere, the Fe-rich samples grown in the partial nitrogen show imperfect texture with various orientations. Even for the $\text{Fe}_{65}\text{Pt}_{35}$ sample grown in the partial nitrogen which show stronger $\{200\}$ texture, the diffractions of $\{001\}$, $\{111\}$, and $\{002\}$ are present. For the Fe-rich films grown in the partial nitrogen flow which show both $\{001\}$ and $\{200\}$ diffraction peaks in the film plane, the large misorientation of neighboring grains from a more random structure would get a large-angle grain boundary, which will act efficiently as pinning sites. This is also why the coercivity drastically decreases for the continuous epitaxial films because a stronger preferred orientation would weaken the pinning effects of domain walls.^{11,12} However, $\text{Fe}_{50}\text{Pt}_{50}$ in both argon and nitrogen are nearly random. The different effects of nitrogen flow on the $\text{Fe}_{50}\text{Pt}_{50}$ and $\text{Fe}_{44}\text{Pt}_{56}$ thin films are discussed as follows.

It has been demonstrated that the coercivity of FePt films increases with the volume fraction of the ordered phase with respect to the disordered phase. The $\text{Fe}_{50}\text{Pt}_{50}$ film grown in nitrogen flow exhibits a heterogeneous structure, in which some smaller grains aggregate. The random anisotropy theory predicts that the aggregation of the small grains would deteriorate the coercivity due to exchange averaging of magnetocrystalline anisotropy and easy formation of reverse domains.²⁶ From the above results, some $L1_2\text{FePt}_3$ phase would be obtained for the $\text{Fe}_{50}\text{Pt}_{50}$ film by the partial nitrogen flow and a large amount of $L1_2\text{FePt}_3$ phase was formed in the $\text{Fe}_{44}\text{Pt}_{56}$ film grown under the partial nitrogen flow. The nitrogen flow is thought to result in a local composition fluctuation to the Pt region, which was confirmed by energy dispersive x-ray spectroscopy and energy filter element map for the film $\text{Fe}_{50}\text{Pt}_{50}$ grown in the partial nitrogen flow. By using energy dispersive x-ray spectroscopy, it was found that the nominal average compositions are similar for the films grown in the argon atmosphere and the partial nitrogen flow. So it can be deduced that the local compositional fluctuation during annealing is mainly due to the releasing of N atoms. Apparently the N atoms have stronger binding with Fe. It was also reported that the frequency factor D_0

samples were investigated for the $\text{Fe}_{100-x}\text{Pt}_x$ thin films ($x = 44, 50, 56, 60,$ and 65). An enhancement of coercivity was achieved by introducing nitrogen during sputtering for the thin films with Fe-rich compositions. But the coercivity of the $\text{Fe}_{50}\text{Pt}_{50}$ and $\text{Fe}_{44}\text{Pt}_{56}$ thin films was deteriorated by nitrogen flow during sputtering. The following are the explanations:

- (1) For the $\text{Fe}_{50}\text{Pt}_{50}$ film, the nitrogen flow makes the microstructure less homogeneous, creating some regions with smaller grain aggregation that is harmful for the magnetic hardness due to the averaging effect of magnetocrystalline anisotropy.
- (2) For the $\text{Fe}_{50}\text{Pt}_{50}$ and $\text{Fe}_{44}\text{Pt}_{56}$ thin films grown in the partial nitrogen, the formation of antiferromagnetic $L1_2\text{FePt}_3$ phases decreases the volume fraction of $L1_0$ -ordered phases, which deteriorates the magnetic properties of thin films.
- (3) For the thin films with Fe-rich compositions, nitrogen flow caused the enhancements of the degree of order and strong preferential in-plane alignment of the c axis, resulting in the enhancement of in-plane coercivity.
- (4) Compared with the Fe-rich films grown in the argon atmosphere which show a strong preferred orientation of $\{111\}$ in the film plane, more randomly oriented nanograin structure in the films with the nitrogen flow is useful for coercivity enhancement due to the more effective pinning of the domain wall.
- (5) Due to coarse structures, the coercivity of the stoichiometric $\text{Fe}_{50}\text{Pt}_{50}$ sample is lower than the one of the $\text{Fe}_{56}\text{Pt}_{44}$ sample.
- (6) By introducing nitrogen during sputtering, the highest coercivity of 1303.0 kA/m was obtained in the $\text{Fe}_{56}\text{Pt}_{44}$ sample, which suggests a promising method of reactive sputtering to improve the magnetic properties of Fe–Pt thin-film systems.

ACKNOWLEDGMENTS

This work was partly supported by the Special Coordination Funds for Promoting Science and Technology on “Nanohetero Metallic Materials” from the Ministry of Education, Culture, Sports, Science and Technology. The authors would like to express thanks to T. O. Seki and Dr. J. Zhang for the help in sample preparation and measurements and the valuable discussions.

- ¹O. A. Ivanov, L. V. Solina, V. A. Demshina, and L. M. Magat, *Phys. Met. Metallogr.* **35**, 81 (1973).
- ²S. W. Yung, Y. H. Chang, T. J. Lin, and M. P. Hung, *J. Magn. Magn. Mater.* **116**, 411 (1992).
- ³J. P. Liu, C. P. Luo, Y. Liu, and D. J. Sellmyer, *Appl. Phys. Lett.* **72**, 483 (1998).
- ⁴H. S. Ko, A. Perumal, and S.-C. Shin, *Appl. Phys. Lett.* **82**, 2311 (2003).
- ⁵C. P. Luo, Z. S. Shan, and D. J. Sellmyer, *J. Appl. Phys.* **79**, 4899 (1996).
- ⁶Y. K. Takahashi, T. Koyama, M. Ohnuma, T. Ohkubo, and K. Hono, *J. Appl. Phys.* **95**, 2690 (2004).
- ⁷T. Ichitsubo, K. Tanaka, M. Koujina, M. Kawashima, and M. Hirao, *Jpn. J. Appl. Phys., Part 1* **43**, 273 (2004).
- ⁸M. Watanabe and M. Homma, *Jpn. J. Appl. Phys., Part 2* **35**, L1264 (1996).
- ⁹M. H. Hong, K. Hono, and M. Watanabe, *J. Appl. Phys.* **84**, 4403 (1998).
- ¹⁰T. Goto, Y. Ide, K. Kikuchi, K. Watanabe, J. Onagawa, H. Yoshida, and J. M. Cadogan, *J. Magn. Magn. Mater.* **177–181**, 1245 (1998).
- ¹¹T. Shima, K. Takanashi, Y. K. Takahashi, and K. Hono, *Appl. Phys. Lett.* **81**, 1050 (2002).
- ¹²S. Okamoto, O. Kitahkumi, N. Kikuchi, T. Miyazaki, Y. Shimada, and Y. K. Takahashi, *Phys. Rev. B* **67**, 094422 (2003).
- ¹³Y. K. Takahashi, T. O. Seki, K. Hono, T. Shima, and K. Takanashi, *J. Appl. Phys.* **96**, 475 (2004).
- ¹⁴M. Watanabe, T. Masumoto, D. H. Ping, and K. Hono, *Appl. Phys. Lett.* **76**, 3971 (2000).
- ¹⁵D. H. Ping, M. Ohnuma, K. Hono, M. Watanabe, T. Iwasa, and T. Masumoto, *J. Appl. Phys.* **90**, 4708 (2001).
- ¹⁶H. Y. Wang, W. H. Mao, X. K. Ma, H. Y. Zhang, Y. B. Chen, Y. J. He, and E. Y. Jiang, *J. Appl. Phys.* **95**, 2564 (2004).
- ¹⁷A. Cebollada, R. F. C. Farrow, and M. F. Toney, in *Magnetic Nanostructures*, edited by H. S. Nalwa (American Scientific, Stevenson Ranch, CA, 2002), p. 95.
- ¹⁸J. S. Chen, B. C. Lim, and J. P. Wang, *Appl. Phys. Lett.* **81**, 1848 (2002).
- ¹⁹V. Karanasos, I. Panagiotopoulos, D. Niarchos, H. Okumura, and G. C. Hadjipanayis, *Appl. Phys. Lett.* **79**, 1255 (2001).
- ²⁰D. Kohler, *J. Appl. Phys.* **31**, 408S (1960).
- ²¹T. Seki, T. Shima, K. Takanashi, Y. Takahashi, E. Matsubara, and K. Hono, *Appl. Phys. Lett.* **82**, 2461 (2003).
- ²²R. Sakurai, Y. Yamamoto, C. C. Chen, M. Hahimoto, J. Shi, Y. Nakamura, and O. Nittono, *Thin Solid Films* **459**, 208 (2004).
- ²³(International Centre of Diffraction Data) Powder Diffraction, JCPDS 43-1359 (unpublished).
- ²⁴H. H. Hsiao, R. N. Panda, J. C. Shih, and T. S. Chin, *J. Appl. Phys.* **91**, 3145 (2002).
- ²⁵H. Okamoto, in *Binary Alloy Phase Diagrams*, edited by Massalski, B. Thaddeus (Published by W. W. Scott, Jr., Ohio, 1990), p. 1752.
- ²⁶G. Herzer, *IEEE Trans. Magn.* **25**, 3329 (1989).
- ²⁷S. Mitani, K. Takanashi, M. Sano, H. Fujimori, A. Osawa, and H. Nakajima, *J. Magn. Magn. Mater.* **148**, 163 (1995).
- ²⁸P. Kamp, *Phys. Rev. B* **59**, 1105 (1999).
- ²⁹S. S. A. Razeq, J. B. Staunto, B. Ginatempo, E. Bruno, and F. J. Pinski, *Phys. Rev. B* **64**, 014411 (2001).
- ³⁰*Diffusion in Solid Metals and Alloys*, LandoltBoernstein New Series Group III, edited by H. Mehrer (Springer, Berlin, 1990), Vol. 26, p. 234.
- ³¹J. Lyubina, O. Gutfleisch, K. H. Müller, L. Schultz, and N. M. Dempsey, *J. Appl. Phys.* **95**, 7474 (2004).
- ³²K. Watanabe and H. Masumoto, *Trans. Jpn. Inst. Met.* **24**, 627 (1983).
- ³³Y. Tanaka, N. Kimura, K. Hono, K. Yasuda, and T. Sakurai, *J. Magn. Magn. Mater.* **170**, 289 (1997).